Research Article
Derivation of Bathymetry Models for Shallow Water Using Multispectral Sentinel-2A Images for Delta Coast of Egypt

[1]Hala M. Ebaid, [2]Dina S. Abdalla and [2]Mohammed A. Soliman
[1]Survey Research Institute, National Water Research Center, Delta Barrages, El-Kanter,
[2]Coastal Research Institute, National Water Research Center, Alexandria Egypt

Abstract: The main objective of this research is to evaluate the effect of sentinel multispectral images on estimating shallow water depth using linear bathymetry model. Multispectral image data was integrated with available echo sounding and GPS data for the determination of the bathymetry after tide correction in three areas on Delta coast i.e., Kitchiner, Damietta and Rashid. Three visible and one near infrared band (Top of Atmospheric Reflectance level, with 10 m resolution) were used in models derivation. Sentinel image bands were geometrically and atmospherically corrected and sun glint was removed prior to bathymetry models estimation. Three models with ln function were the derivates using Ordinary Least Square (OLS) modeling tool under ArcGIS environment. The results indicated that Adjusted R-Squared for the three estimated bathymetry models were 0.68, 0.62 and 0.72 for Damietta, Rashid and Kitchiner areas respectively. About 75% of the residual values ranged from -1.63 to 1.3 m for Damietta points and 50% of the residual values were between -0.39 to 0.57 m for Rashid and about 65% between -0.76 to 0.97 m for Kitchiner. Hence it can be concluded that these predicted models provide time- and cost-effective solution for Shallow water depths estimation.

Keywords: Bathymetry, delta coast of Egypt, ordinary least square, sentinel-2A images

INTRODUCTION

Bathymetry information is one of the important parameters which plays a major role in planning near-shore structure activities such as engineering work, pipeline laying, port management and dredging operation. It is also significantly important to determine the underwater topography, movement of sediments and to generate the hydrographic chart for safety transportation. Monitoring batihymetry throughout the year is essential for sediment level prediction to maintain smooth navigation. The traditional bathymetric surveying of shallow sea water based on ship-borne echo sounding operations is costly and time consuming, where a dense network of measured points is required. On the other hand remotely sensed data have provided a cost-and time-effective solution to accurate depth estimation (Lyzenga, 1985; Stumpf et al., 2003; Su et al., 2008).

In the following years, the advance of remote sensing technology expanded the use of these methodologies to data with improved spatial and spectral resolution, like Ikonos (Stumpf et al., 2003; Mishra et al., 2004; Su et al., 2008), Quickbird (Conger et al., 2006; Lyons et al., 2011) and Worldview-2 data

(Kerr, 2011; Bramante et al., 2013). The main hindrances while applying these processes were reflectance penetration and water turbidity (Conger et al., 2006; Su et al., 2008; Negm et al., 2016). However, the bathymetric approaches involving satellite imagery data are regarded as a fast and economically advantageous solution to automatic water depth calculation in shallow water (Stumpf et al., 2003; Su et al., 2008).

A wide variety of empirical models has been evaluated for bathymetric by applying relationship between image pixel values and field-measured water depth values. The popular approach was examined by Lyzenga (1978, 1981, 1985) and was based on the bottom-reflected reflectance is approximately a linear function of the bottom reflectance and an exponential function of the water depth. Stumpf et al. (2003) presented an algorithm using a ratio of reflectance and demonstrated its benefits to retrieve depths even in deep water (>25 m) contrary to standard linear transform algorithm. Moreover, a modified version of Lyzenga's model has been proposed by Conger et al. (2006) employing a single color band and LIDAR bathymetry data rather than two color bands in rotating process.

Corresponding Author: Hala M. Ebaid, Survey Research Institute, National Water Research Center, Delta Barrages, El-Kanter, Egypt

The main objective of this research is to evaluate the effect of sentinel multispectral images on estimating shallow water depth using linear bathymetry model. This study was, therefore, undertaken to:

- Evaluate the contribution of visible and near infrared bands of sentinel-2A imagery in estimating shallow water bathymetry for the three study areas along the delta coast of Egypt
- Derivate the linear bathymetric models using echo sounding data for calibration
- To study the effect of both sun glint removal and atmospheric correction on imagery data and in turn on shallow water bathymetry model performance.

Linear bathymetric model: The relationship between an observed reflectance R_w and the corresponding water depth z and bottom reflectance A_d is described by Lyzenga (1978) as Eq. (1):

$$R_w = (A_d - R_w) \exp(-gz) + R_{dp} \qquad (1)$$

where,
R_{dp} = Dark pixel value
g   = A function of the attenuation coefficients.

Rearranging Eq. (1) depth z can be described as Eq. (2) (Stumpf et al., 2003):

$$Z = g^{-1}[\ln(A_d - R_w) - \ln(R_w - R_{dp})] \qquad (2)$$

where, $(R_w - R_{dp})$ is +ve

The method of single band for depth estimation assumes that the bottom is homogeneous and the water quality is uniform for the whole study area. Lyzenga (1978, 1985) explained that using two bands could correct the errors coming from different bottom types considered that the ratio of the bottom reflectance between the two bands for all bottom types is constant over all scene pixels. According to this idea the proposed model is described in Eq. (3) (Lyzenga, 1985):

$$Z = a_0 + a_i X_i + a_j X_j \qquad (3)$$

where,
$X_i = \ln(R_{wi} - Rd_{pi})$
$X_j = \ln(R_{wj} - Rd_{pj})$

Paredes and Spero (1983) proved that if there are at least as many bands as the existing bottom types in a study area, an independent from bottom types depth can be estimated. Lyzenga et al. (2006) proved that the n-band model:

$$Z = a_0 + \sum_{i=1}^{i=n} a_i x_i \qquad (4)$$

where, X_i is described above, although derived under the assumption that the water optical properties are uniform (Lyzenga, 1978, 1985) gives depths that are not influenced by variations in water properties and/or bottom reflectance. This means that the more the available bands are, the better the depth estimation. According to Bramante et al. (2013) imagery data with multiplicity of bands should produce better results over heterogeneous study areas. From which this study will support this technique which based on Eq. (4).

STUDY AREA AND DATA USED

Models were carried out to estimate the depth of water for three study areas along the coast of Egypt. The three coastal areas are Damietta, which lies in the eastern part of the coast is about 9 km length and 1.5 width; Rashid in the west with 7 km length and 1.2 km width; Kitchiner, lying in between is 8 km length and 1.6 km width as demonstrated in Fig. 1. These three study areas were chosen (due to availability). The sea bottom changes smoothly and water is clear, besides that the shallower and the deeper water areas are sandy for all study areas.

Sentinel -2A images is Level-1C product (orthorectified TOA reflectance) were used in this study. The imagery dataset used includes four bands, with spatial resolution 10 m: blue (490 nm), green (560 nm), red (665 nm) and near-infrared (842 nm). The images were acquired in 19 September 2016. Despite the water clarity, the depths estimation was constrained by image noise that sun glint caused by appearing

Fig. 1: Three study areas along Delta coast

sparsely in a great part of image scene. The bathymetric model was calibrated using echo-sounding data. The survey of the sea bottom was partly accomplished using 12325, 3699 and 27415 measurements of depths that ranged from -11.7 m to 2.6 m for the three coastal study areas i.e., Damietta, Rashid and Kitchiner, respectively; beside using the GPS which corresponds to a horizontal position on the sea surface. The in situ echo-sounding data was collected by the (Coastal Research Institute (CORI), data reports 2015, 2013, 2016). Fotiou and Pikridas (2006) reported that the internal accuracy of depth measurements reached 10cm and the horizontal position as determined using the kinematic method showed a final accuracy of 5-6 cm. All data process was performed using manufacturer processing software, while the multispectral dataset was georeferenced to the system of the horizontal coordinates for the depth points.

METHODOLOGY

Imagery data pre-processing: The multispectral data (2, 3, 4, 8 bands) were layer stacked then georeferenced to UTM (zone 36) system and WGS84. Deglinting and atmospheric correction processes were made for every band to evaluate their effect on estimated depth values. The available sun glint removal methods are categorized depending on the applied water location and condition, either open ocean or shallow waters. Kay *et al*. (2009) provide a thorough review of deglinting methodologies. A popular one for shallow waters deglinting was proposed by Hochberg *et al*. (2003) and was based on the exploitation of the linear relationships between Near Infra-Red band (NIR) and every other visible bands of the sentinel images in a linear regression by using samples of isolated pixels from the whole image. Hedley *et al*. (2005) simplified the implementation of this method and made it more robust by using samples of image pixels. The effectiveness of this method relies on choice of the darkness pixel samples, reasonably deep and with evident glint (Green *et al*., 2000, Hedley *et al*., 2005, Edwards, 2010). The linear regression runs between the sample pixels of every visible band on y-axis and the corresponding pixels of NIR band on x axis. All the image pixels are deglinted according to Eq. (5) by (Hedley *et al*., 2005):

$$R'_i = R_i - b_i (R_{NIR} - Min_{NIR}) \tag{5}$$

where,
R'_i = The deglinted pixel value
R_i = The initial pixel value
b_i = The regression line slope
R_{NIR} = The corresponding pixel value in NIR band
Min_{NIR} = The minimum NIR value existing in the sample

The technique of Hedley *et al*. (2005) was applied in this study on the 'glint' image bands towards the
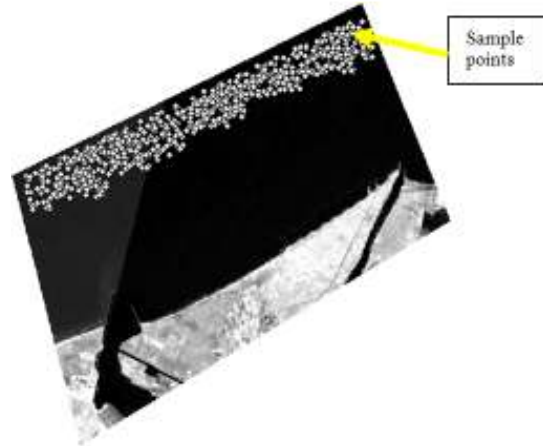

Fig. 2: Damietta coastal area with sample points for deglinted pixel of green visible band
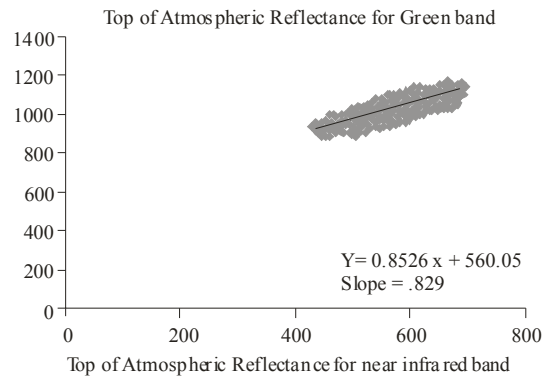

Fig. 3: Damietta coastal area with sample points for deglinted pixel of green visible ban

correction of sun-glint effect. Figure 2 and 3 describes the sample points and the deduced slope between green band and near infrared band for Damietta region (as an example). By applying extract multi values to Points tool (under Spatial Analyst toolset), cell values will be extracted at associated sample points locations for all raster bands and these values will be recorded to the attribute table of the resulted point feature class of raster values.

After the glint correction, different atmospheric correction algorithm were tried in this study as follows:

- Dark Object Subtraction (DOS), which is considered as the simplest way for atmospheric correction. In order to avoid negative differences between the image pixels and the dark pixel value, the histogram of every band was examined and a cut-off at its lower end was spotted. The value corresponding to this cut-off was considered as the dark pixel value (Benny and Dawson, 1983).
- Sentinel-2 ATCOR under PCI Geomatics environment to turn TOA reflectance into Bottom-Of-Atmospheric (BOA) reflectance. All algorithm

concerning different atmospheric information as aerosol type and climate condition, visibility map parameters, also haze and cloud masking parameters were applied. All these atmospheric correction algorithms and methods do not improve the correlation between estimated and measured depth in all study areas.

Derivation of bathymetry models for the three coastal study areas: The linearity between the measured depth (using hydrographic survey for shallow water of coastal areas for Damietta, Rashid and Kitchiner and the corresponding pixel values (at TOA reflectance level) for every band were firstly evaluated after image geometric correction. And these linearity evaluations were carried out to test the most effective band on estimated depth values. Ordinary Least Square (OLS) regression was carried out between control points of known depth over the three coastal study areas and sentinel images bands: 2(Blue), 3(Green), 4 (Red) and 8(Near infrared). Different bands formulas and bands combinations were investigated and tested for the output model after and before transformation from Top of Atmospheric (TOA) correction to Ground of Atmospheric (GOA) correction and deglinated processes. After sequential statistical tests and outliers values removal, final models were defined.

RESULTS AND DISCUSSION

An increasing number of studies have shown that bathymetric information can be derived from optical satellite multispectral imagery at the spatial resolution of the source image. Various inversion models have been developed to convert image pixel values into depth estimates. The log-linear inversion model developed by Lyzenga (1978) is the most popular among them. Sun glint removal and atmospheric correction of remotely sensed data are essential processes prior to the application of a bathymetry model, as reported by Negm *et al*. (2016).

The coefficient of determination (R^2) between the true measured water depth values after tide correction and the corresponding pixel values for every band (at Top of atmospheric reflectance level) of the three study areas after geometric correction process is clarified in Table 1; where both the red and near-infra red bands showed the highest correlation for the three shallow water study areas. These highest correlation values indicate that these same bands will affect the resulted models for better estimation of depth values.

The estimated model for Damietta area: Ordinary Least Square was carried out using multispectral bands (as independent variables) and 12325 control points (as dependent variable). These in situ measured depths spanned a range between -.4 and -11.7 m (with mean= -

Table 1: The coefficient of determination (R^2) between the measured corrected depth and the corresponding pixel values for each band (B, G, R, NIR) for the three study areas

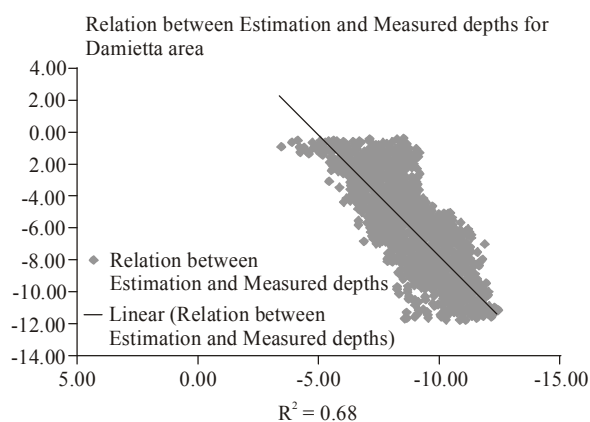| Study areas	Bands	R^2 (Top of atmospheric reflectance)
Damitta	Blue	0.024
	Green	0.021
	Red	0.139
	Near-Infrared	0.244
Rashid	Blue	0.016
	Green	0.046
	Red	0.103
	Near-infrared	0.510
Kitchiner	Blue	0.359
	Green	0.643
	Red	0.696
	Near-Infrared	0.696

Fig. 4: Relation between measured and estimated shallow water depth for Damietta coastal area

5.95 and standard deviation = 2.47). The resulted OLS model for Damietta area is demonstrated as follows:

Y= - 85.19 - 0.037 B+ 3.72 Lndeg_G - 10.56 Lndeg_R + 26.22 Ln_NIR

where,
Y is Estimated depth for Damitta area

Lndeg _G, Lndeg R, are Ln deglinated of Top of Atmospheric Reflectance for, Green and Red. Ln_NIR is Ln Reflectance for Near Infra-red band, B is Top of Atmospheric Reflectance.

Figure 4 describes the linear relation between estimated and measured depth for Damietta coastal area

Ideally the histogram which shows the difference between measured and estimated depth values expressed as resulted standardized residuals would match the normal curve. Figure 5a demonstrates the histogram of Damietta study area which does not look very different from the normal curve, which means that, the model is very little biased.

Figure 5b demonstrates the predicted depth values from model on the x-axis and the accuracy of the prediction on the y-axis; the distance from the line at 0 describes how bad the prediction was for that value.
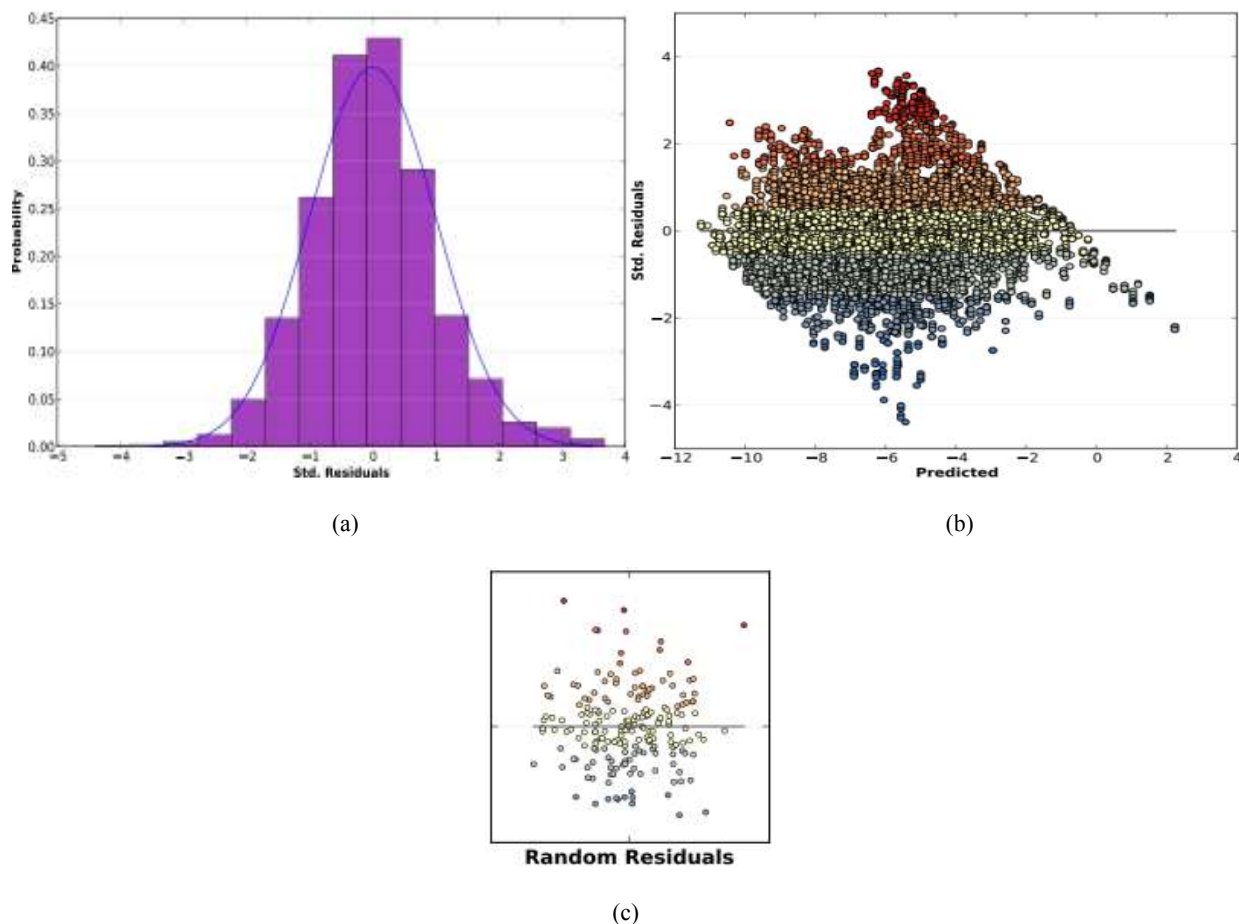
(a)

(b)

(c)

Fig. 5: (a): Histogram of standardized residuals; (b): Residual vs. predicted plot; (c): Random residuals for estimated model for Damietta coastal area

The accuracy of the predicted model is quite good. Figure 5c demonstrates random residual values for Damietta model. It is clear from Fig. 6 and 7, that the highest residual values are for points nearby construction work inside the water, thus realizing the highlighted column of residual values on histogram and the corresponding ones on the image. About 75% of the residual values was between -1.63 and 1.38 m with standard deviation of 0.84.

The output estimated bathymetry map for Damietta coastal area is showed below (Fig. 7).

Rashid area model: Ordinary Least Square was carried out using multispectral bands (as independent variables) and 3699 in situe control points (as dependent variables), with in situe measurements depth spanned a range from -8.3 m to-2.5 m, with mean of -6.15 and standard deviation of 1.09. The resulted OLS model for Rashid coastal area is:

$Y = 18.69 + 0.86$ Lndeg_B $- 6.88$ Lndeg _G $+ 0.344$ Lndeg _R $+ 1.677$ NIR

where,

Y is estimated depth of shallow water for Rashid coastal area

Lndeg_B, Lndeg_G, Lndeg_R are Ln deglinated of Top of Atmospheric Reflectance for Blue, Green and Red. NIR is Near Infra_red reflectance band.

Figure 8 describes the linear relation between estimated and measured depth for Rashid coastal area ($R^2 = 0.62$)

The histogram of Standardized Residuals for Rashid coastal area is approximately taking the shape of normal curve which indicates that the model is also little biased. About 50% of the residual values ranges from -0.39 - 0.57 m. with Standard Deviation of 0.25 m. The accuracy of the predicted model looks reasonable (Fig. 9a and 9b). Figure 9c demonstrates random residual values for Rashid model.

The resulted output of estimated bathymetry map for Rashid coastal area is demonstrated as follows (Fig. 10).

Kitchiner area model: Ordinary Least Square was carried out between multispectral bands (as independent variables) and 27415 in situ control points (as
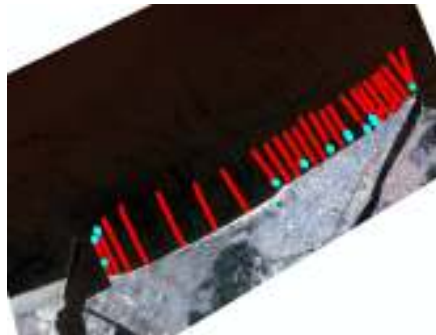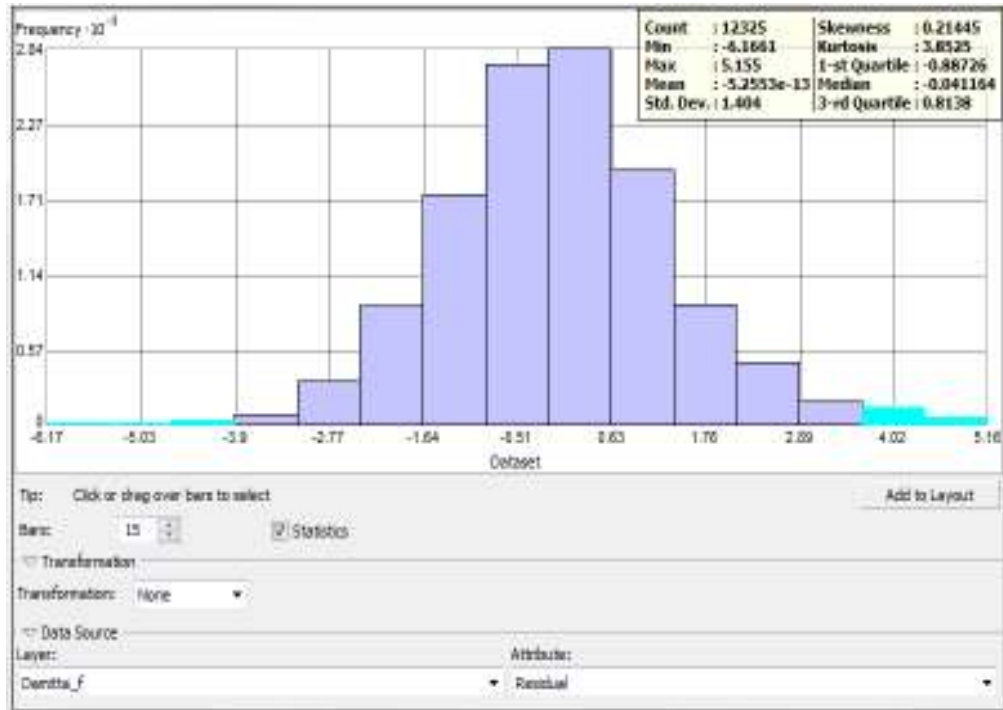
Fig. 6: The positions of highest residual values for Damietta coastal area

Fig. 7: Predicted bathymetry map for Damietta coastal area

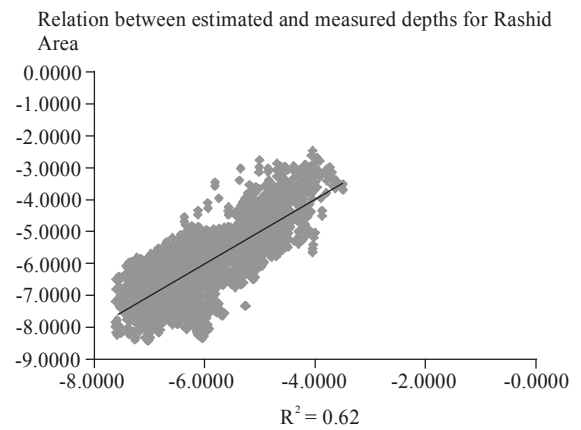Relation between estimated and measured depths for Rashid Area

$R^2 = 0.62$

Fig. 8: Relationship between measured and estimated shallow water depth for Rashid coastal area

dependent variable), with measured depth spanned a range between -7.2 and 2.6 m with mean of -4.01 and
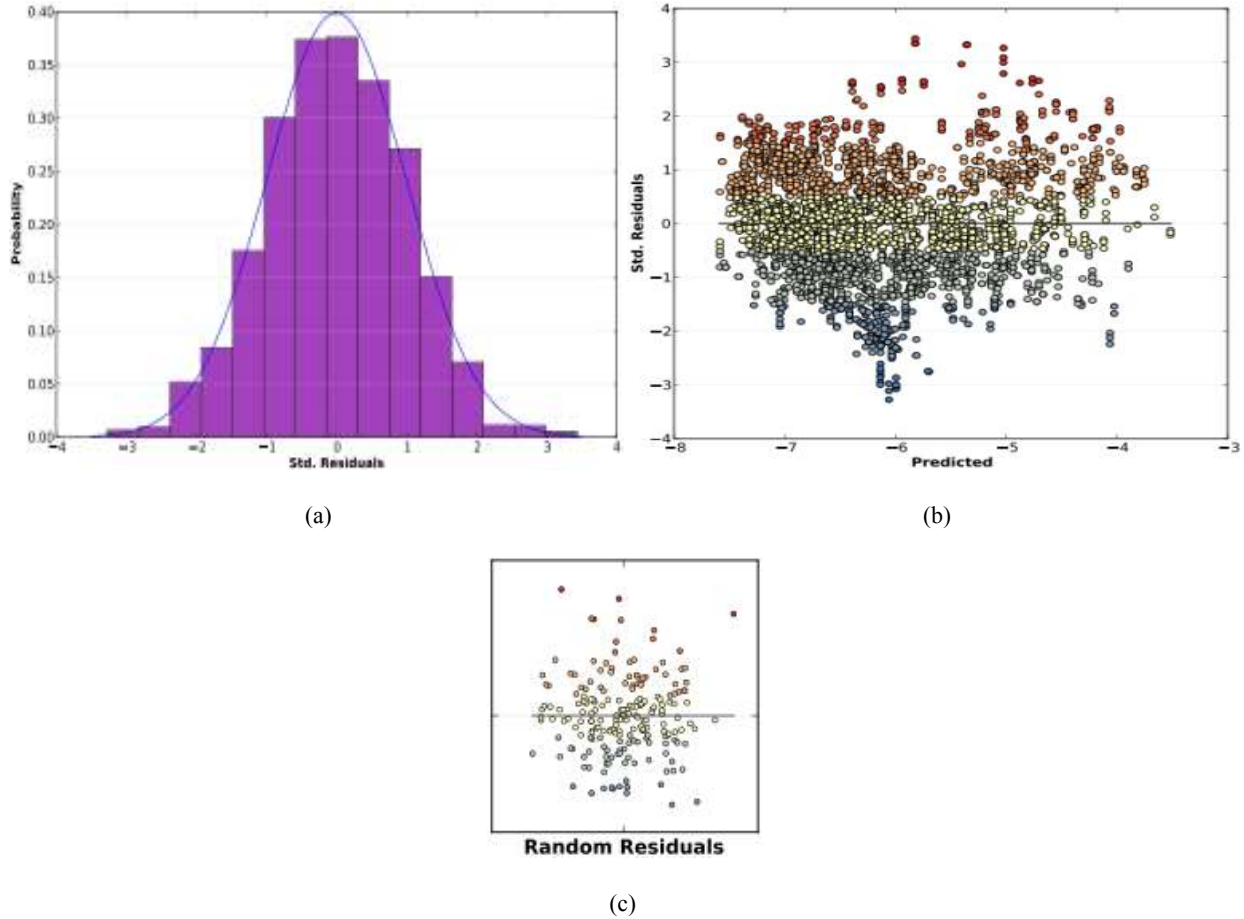
(a)

(b)

Random Residuals

(c)

Fig. 9: (a): Histogram of Standardized Residuals; (b): Residual vs. Predicted Plot; (c): Random residuals for estimated model for Rashid coastal area
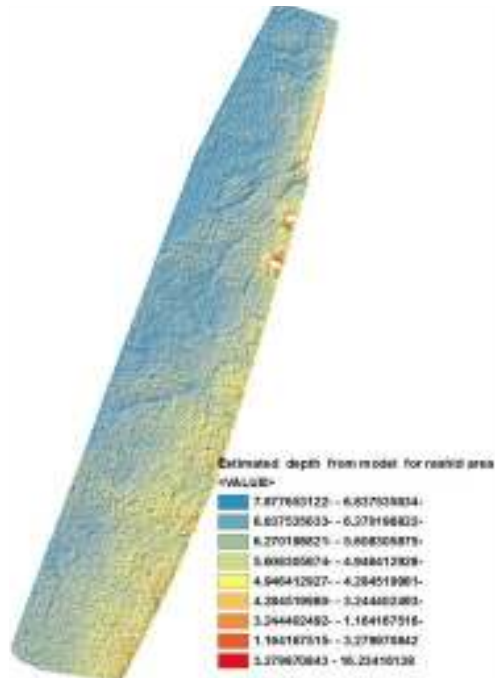

Fig. 10: Predicted bathymetry map for Rashid coastal area

standard deviation of 1.5. The resulted OLS model for kitchiner area is demonstrated as follows:

$$Y= -31.85 + 0.009 \text{ Deg\_B} - 0.002 \text{Deg\_G} + 0.014 \text{ Deg\_R} + 0.019 \text{ NIR}$$

where,
- Y is estimated depth of shallow water for kitchiner area
- Deg_B, Deg_G, Deg_R, are Deglinated Top of Atmospheric Reflectance for blue, green red bands. NIR is near infrared reflectance band.

Figure 11 describes the linear relationship between estimated and measured depth for Kitchiner coastal area ($R^2 = 0.72$)

The histogram of Standardized Residuals for kitchiner coastal area is approximately takeng the shape of normal curve (Fig. 12a) which also indicates very little biased model. About 65% of the residuals range between (-0.76 -0.97) m, with Standard Deviation = 0.33 m. Figure 12b and 12c showed very good accuracy of the predicted kitchiner model.
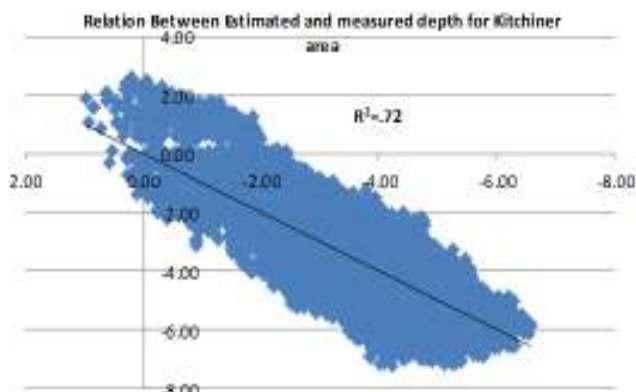
Fig. 11: Relation between measured and estimated shallow water depth for Kitchiner coastal area

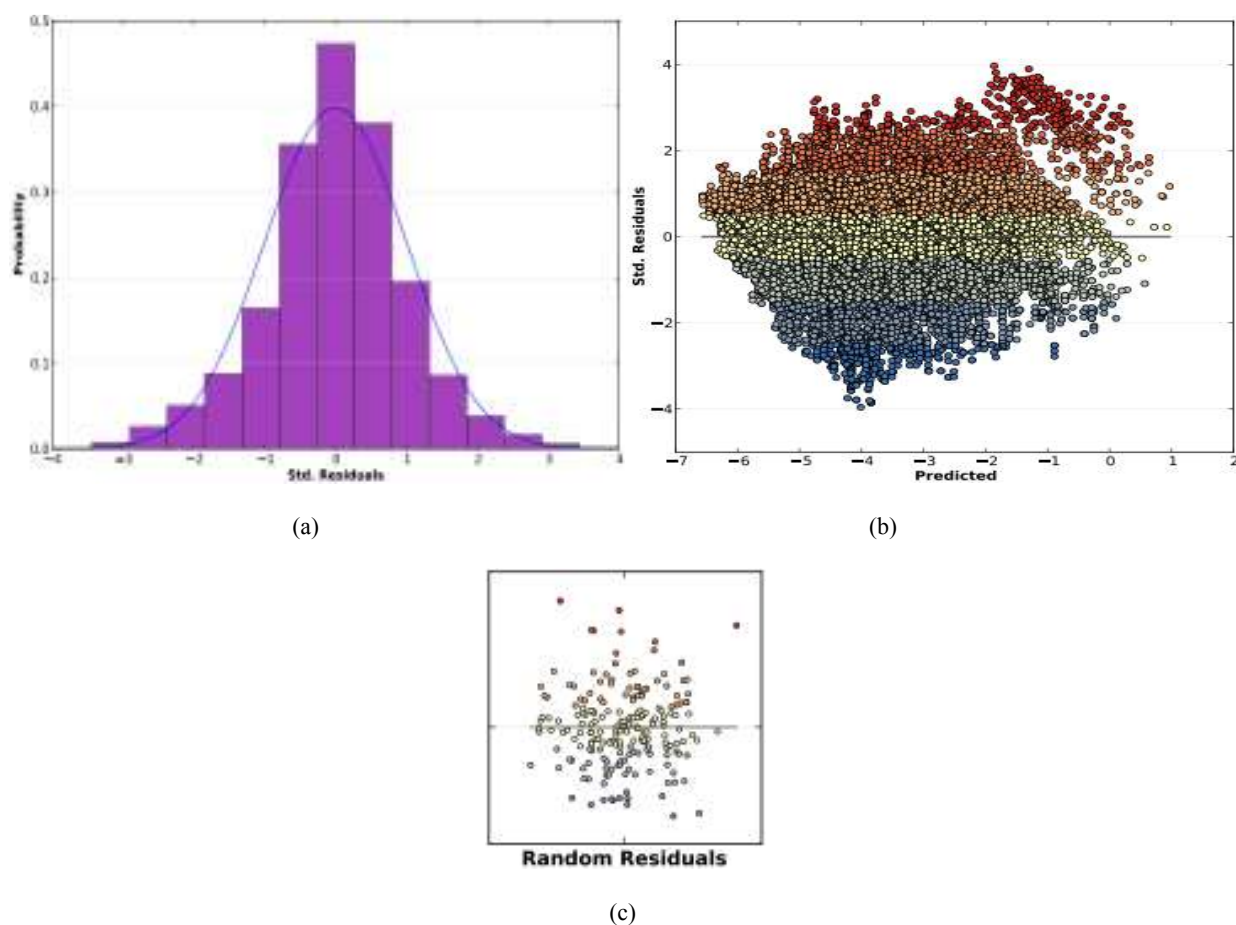(a)   (b)

(c)

Fig. 12: (a): Histogram of standardized residuals; (b): Residual vs. predicted plot; (c): Random residuals for estimated model for Kitchiner coastal area

The resulted output of estimated bathymetry map for Kitchiner coastal area is demonstrated in Fig. 13.

All resulted models gain some source of errors: First the date of Hydrographic in situe measurements is different from the acquisition date of the images (2016), where the depth for Kitchiner area was measured in 2015, while that for Damitta area was measured in 2013. Second the spatial resolution is not sufficient for these specific shallow water areas. Third the accuracy of georeference process of the images affects the overall accuracy of resulted model. Despite of all these source of errors the accuracy and the performance of the resulted models are still quite reasonable.

CONCLUSION

Bands 2(Blue), 3(green), 4(Red) and 8(NIR) of the sentinel image were stacked, then they were
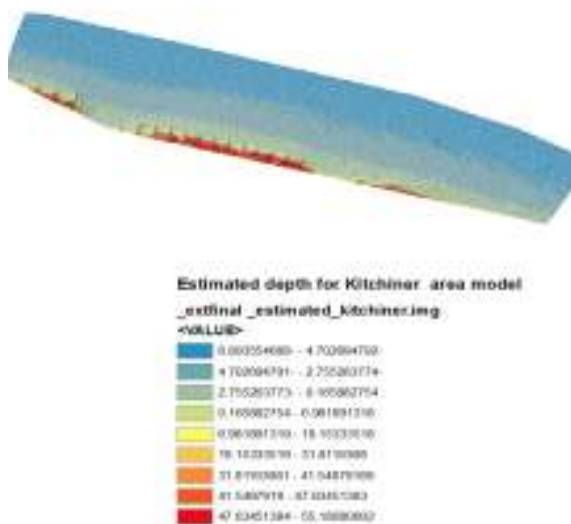
Fig. 13: Predicted bathymetry map for Kitchiner coastal area

geometrically corrected. The linear bathymetric models (using OLS method) were carried out on the image before and after removing sun glint and atmospheric correction to assess their influence on the predicted models. The image bands were integrated with the available echo sounding and GPS data for calibrating the models as well as for the analysis of the corresponding depths in the three study areas i.e., Kitchiner, Rashid and Damietta. Different functions as band combination and band ratio were tested for derivation of optimum models. It was found that using Ln function for most of the bands improved the estimated depth models. Also the outcomes of the statistical analysis indicated that the model provided very good results by integrating the four bands with 10 m resolution in all models. The contribution of NIR and Red bands for the three areas were significant in all models. In this study, all models were improved after sun deglinated process. While atmospheric correction didn't improve the models, despite the trials of different atmspheric correction algorithm such as: Dark Object Subtraction (DOS) and Sentinel-2 ATCOR under PCI Geomatics environment. All algorithm concerning different atmospheric information as aerosol type and climate condition, visibility map parameters, also haze and cloud masking parameters were applied and still didn't improve the correlation between estimated and measured depth. In general, the resulted bathymetric models involving the imagery data of moderate spectral and spatial resolution produced fairly reasonable results. However, a thorough statistical analysis was required to optimize the selection of the appropriate spectral bands. Also efforts are needed to obtaining bathymetry data for the Nile Delta and elsewhere in Egypt. And this study considers as a part of a larger effort to evaluate various cost effective, relatively accurate and practical bathymetry survey methods.

REFERENCES

Benny, A.H. and G.J. Dawson, 1983. Satellite imagery as an aid to bathymetric charting in the Red Sea. Cartogr. J., 20(1): 5-16.

Bramante, J.F., D.K. Raju and S.T. Min, 2013. Derivation of bathymetry from multispectral imagery in the highly turbid waters of Singapore's south islands: A comparative study. Int. J. Remote Sens., 34(6): 2070-2088.

Conger, C.L., E.J. Hochberg, C.H. Fletcher and M.J. Atkinson, 2006. Decorrelating remote sensing color bands from bathymetry in optically shallow waters. IEEE T. Geosci. Remote, 44(6): 1655-1660.

Edwards, A.J., 2010. Lesson 5: Removing sun glint from Compact Airborne Spectrographic Imager (CASI) imagery. Bilko Module 7, UNESCO.

Fotiou, A. and C. Pikridas, 2006. GPS and Geodetic Applications. Ziti, Thessaloniki, Greece.

Green, E.P., P.J. Mumby, A.J. Edwards and C.D. Clark, 2000. Remote Sensing Handbook for Tropical Coastal Management. Ch. 8. Coastal Management Sourcebooks Series. UNESCO Publications, Paris, pp: 219-233.

Hedley, J.D., A.R. Harborne and P.J. Mumby, 2005. Technical note: Simple and robust removal of sun glint for mapping shallow-water benthos. Int. J. Remote Sens., 26(10): 2107-2112.

Hochberg, E.J., S. Andrefouet and M.R. Tyler, 2003. Sea surface correction of high spatial resolution Ikonos images to improve bottom mapping in near-shore environments. IEEE T. Geosci. Remote, 41(7): 1724-1729.

Kay, S., J.D. Hedley and S. Lavender, 2009. Sun glint correction of high and low spatial resolution images of aquatic scenes: A review of methods for visible and near-infrared wavelengths. Remote Sens., 1(4): 697-730.

Kerr, J.M., 2011. WorldView-02 offers new capabilities for the monitoring of threatened coral reefs. Digital Globe 8Band Challenge Winner.

Lyons, M., S. Phinn and C. Roelfsema, 2011. Integrating Quickbird multi-spectral satellite and field data: Mapping bathymetry, seagrass cover, seagrass species and change in Moreton Bay, Australia in 2004 and 2007. Remote Sens., 3: 42-64.

Lyzenga, D.R., 1978. Passive remote sensing techniques for mapping water depth and bottom features. Appl. Optics, 17(3): 379-383.

Lyzenga, D.R., 1981. Remote sensing of bottom reflectance and water attenuation parameters in shallow water using aircraft and Landsat data. Int. J. Remote Sens., 2(1): 71-82.

Lyzenga, D.R., 1985. Shallow-water bathymetry using combined lidar and passive multispectral scanner data. Int. J. Remote Sens., 6(1): 115-125.

Lyzenga, D.R., N.P. Malinas and F.J. Tanis, 2006. Multispectral bathymetry using a simple physically based algorithm. IEEE T. Geosci. Remote, 44(8): 2251-2259.

Mishra, D., S. Narumalani, M. Lawson and D. Rundquist, 2004. Bathymetric mapping using IKONOS multispectral data. GISci. Remote Sens., 41(4): 301-321.

Negm, A.M., H. Mohamed, M. Zahran and S. Abdel-Fattah, 2016. Estimation of Bathymetry Using High-resolution Satellite Imagery: Case Study El-Burullus Lake, Northern Nile Delta. In: Negm, A. (Ed.), The Nile Delta. The Handbook of Environmental Chemistry. Springer, Cham, 55: 425-454.

Paredes, J.M. and R.E. Spero, 1983. Water depth mapping from passive remote sensing data under a generalized ratio assumption. Appl. Optics, 22(8): 1134-1135.

Stumpf, R.P., K. Holderied and M. Sinclair, 2003. Determination of water depth with high-resolution satellite imagery over variable bottom types. Limnol. Oceanogr., 48(1): 547-556.

Su, H., H. Liu and W.D. Heyman, 2008. Automated derivation of bathymetric information from multi-spectral satellite imagery using a non-linear inversion model. Mar. Geod., 31(4): 281-298.